Breast imaging using an LED-based photoacoustic and ultrasound imaging system: a proof-of-concept study

Kuniyil Ajith Singh, Mithun, Dantuma, Maura, Kalloor Joseph, Francis, Manohar, Srirang, Steenbergen, Wiendelt

Mithun Kuniyil Ajith Singh, Maura Dantuma, Francis Kalloor Joseph, Srirang Manohar, Wiendelt Steenbergen, "Breast imaging using an LED-based photoacoustic and ultrasound imaging system: a proof-of-concept study," Proc. SPIE 11642, Photons Plus Ultrasound: Imaging and Sensing 2021, 116420G (5 March 2021); doi: 10.1117/12.2578590

SPIE.

Event: SPIE BiOS, 2021, Online Only

Breast imaging using an LED-based photoacoustic and ultrasound imaging system: a proof-of-concept study

Mithun Kuniyil Ajith Singh*[a], Maura Dantuma[b], Francis Kalloor Joseph[c], Srirang Manohar[b], and Wiendelt Steenbergen[c]
[a]Research & Business Development Division, CYBERDYNE INC, Cambridge Innovation Center, Rotterdam, the Netherlands,
[b]Multi-Modality Medical Imaging (M3I) group, TechMed Centre, University of Twente, Enschede, the Netherlands
[c]Biomedical Photonic Imaging group, TechMed Centre, University of Twente, Enschede, the Netherlands
*Email: mithun_ajith@cyberdyne.jp; Phone: +31108080827; Website: https://www.cyberdyne.jp/english/

ABSTRACT

Photoacoustic imaging holds potential in diagnosis and treatment monitoring of breast cancer, but clinical translation of this technology has often been hindered by bulky and expensive excitation sources. In this work, the potential of a portable, dual-mode multispectral LED-based photoacoustic and ultrasound system (AcousticX) in breast imaging is investigated for the first time. The AcousticX system comprises a linear array ultrasound probe (7 MHz) and two dual-wavelength LED arrays (750/850 nm) placed on both sides of the probe. Two experiments were performed to investigate the potential of the system in imaging the breast. In the first instance, interleaved photoacoustic and ultrasound imaging was performed on a semi-anthropomorphic multi-layered 3D breast phantom with possibility to tune oxygen saturation in blood vessel structures. In the second experiment, vasculature of a healthy human breast was imaged *in vivo*. Skin and multiple vascular features along with its relative oxygen saturation are visualized using photoacoustic imaging and the ultrasound images offered valuable structural information including fat, fibroglandular tissue and pectoral muscles. In human *in vivo* experiments, we achieved an imaging depth of around 1.7 cm at a display frame rate of 10 Hz, the highest *in vivo* imaging depth reported in LED-based photoacoustic imaging using a 7 MHz probe. With the capability of providing real-time structural and functional information, AcousticX holds clinical translation potential in non-invasive breast imaging.

Keywords: LED, photoacoustic imaging, ultrasound imaging, breast cancer, hypoxia, tumour

1. INTRODUCTION

Breast cancer is a significant public health problem with huge societal and economic impact. It is the most frequently occurring malignancy with 2.3 million new cases (11.7 % of all diagnosed cancer cases) in 2020[1]. In future, breast cancer incidence and mortality in developed countries are expected to be stabilized. However, developing and under-developed countries foresee a steep growth of cases in coming years[2]. Imaging plays an important role in the entire breast cancer management path, spanning from detection to guidance of surgeries[3]. Gold standard modalities for breast imaging are X-ray mammography, ultrasound (US) imaging and Magnetic Resonance imaging (MRI), each with its own advantages and disadvantages. Sensitivity and specificity of X-ray mammography and US imaging are reported to be non-optimal. Use of ionizing radiation, poor imaging performance in dense breasts, and painful compression are the major problems associated with X-ray mammography, the most common breast cancer imaging technique[4]. US imaging is capable of giving real-time structural and morphological information about breast tumours with high resolution. However, operator variability in acquired images and false positive rates are important concerns when using US imaging[5]. Contrast-enhanced MRI is an excellent imaging modality with possibility to image tumour vasculature with high resolution. However, requirement of contrast agents, high cost, and low specificity are the issues associated with this modality in breast cancer imaging[6]. Early detection is the key and a cost-effective handheld non-invasive breast scanner with high sensitivity and specificity, which is suitable for resource-limited settings is expected to have huge impact globally.

Photons Plus Ultrasound: Imaging and Sensing 2021, edited by Alexander A. Oraevsky
Lihong V. Wang, Proc. of SPIE Vol. 11642, 116420G · © 2021 SPIE
CCC code: 1605-7422/21/$21 · doi: 10.1117/12.2578590

Angiogenesis, the growth of vasculature to support the development of invasive tumours, is one of the important characteristics of cancer[7]. Angiogenesis results in enhanced blood vessel density and hypoxia (low blood oxygen saturation) at tumour sites because of the cancer's outgrowth of existing neo-vasculature. Abnormal blood vessel density and hypoxia in and around tumour may be an early marker for breast cancer. Since haemoglobin offers excellent optical spectroscopic contrast, light-based imaging modalities hold good potential in breast imaging, especially when contrast agents are used to enhance the imaging depth[8]. However, pure optical imaging methods offer poor spatial resolution because of high light scattering in breast tissue.

Photoacoustic (PA) or optoacoustic imaging is a hybrid modality which offers a rare combination of optical spectroscopic contrast and ultrasonic resolution and imaging depth[9]. Breast imaging is one of the most important and most explored clinical applications of PA imaging[10]. Functional parameters like increased blood vessel density (even without blood flow) and reduction in blood oxygen saturation (sO_2) in and around deep-seated tumours can be detected with high resolution using PA imaging. Pulse-echo US, one of the most common imaging modalities in clinics is capable of providing structural and morphological details of breast tumours[5]. In addition, blood flow information in bigger blood vessels can also be obtained using US-based Doppler methods. Since both PA and US imaging relies on acoustic detection, it is possible to combine these two modalities in a portable scanner offering structural, morphological and functional information in real-time 2D measurements[11]. US imaging is a well-accepted clinical modality, and it is expected that addition of PA imaging to this will have easier clinical acceptance and accelerate clinical translation. Combined laser-based PA and US imaging systems has shown good potential in distinguishing breast cancer molecular subtypes[12]. However, the bulky, slow and expensive pulsed lasers used in these systems are not ideal in a resource limited clinical setting[13]. Requirement of laser-safe rooms and eye safety goggles may not be ideal when installing such a system in hospital. Owing to its portability, affordability and ease-of-use, use of LED's as an alternate illumination source in PA imaging has been studied extensively in recent years[14-22].

In this proof-of-concept work, the potential of a portable and affordable multispectral LED-based PA and US system (AcousticX, CYBERDYNE INC, Tsukuba, Japan) in breast imaging is investigated for the first time. By performing real-time interleaved dual-wavelength PA and US imaging on realistic breast phantoms and a human volunteer, we validate the scope of combined LED-based PA and US in breast imaging.

2. MATERIALS AND METHODS

2.1 Equipment and setup

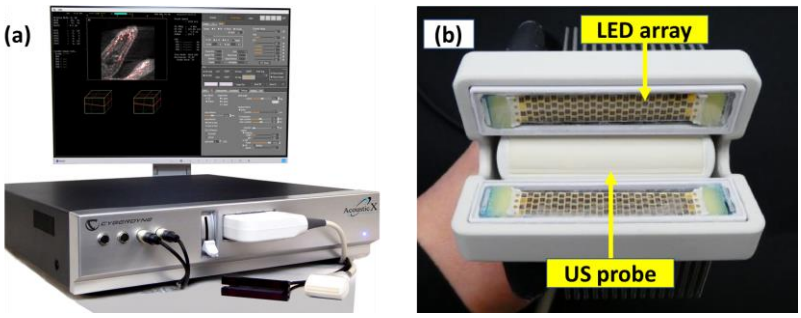

Figure 1. (a) Photograph of commercial dual-wavelength LED-based PA/US imaging system (AcousticX) and (b) details of arrangement of LED arrays on both sides of US probe. Custom-made gel-pad is used to fill the gap between LED arrays and US probe to enable a completely handheld operation during human *in vivo* experiments.

For both phantom and *in vivo* human volunteer experiments, we used the commercially available multispectral LED-based PA/US imaging system (AcousticX, CYBERDYNE Inc, Tsukuba, Japan)[19,20] (Fig. 1a). This portable system with a handheld probe (Fig. 1b) is capable of providing real-time interleaved LED-PA, US, and sO_2 images with a maximum frame rate of 30 Hz. In all experiments, we used 7 MHz linear array US probe (128 elements, fractional bandwidth: 77%) for acoustic detection. Illumination was provided by two dual-wavelength LED arrays (wavelength: 750/850 nm, pulse energy: 100/200 µJ per pulse, pulse width: 70 ns) placed on both side of the US probe. These arrays are capable of switching between wavelengths at a rate of 4 KHz, which helps in reducing the motion-related artifacts during dual-wavelength PA imaging. Pulse repetition rate (PRF) of the system is 4 KHz and there is ample time available to average multiple frames without compromising on temporal resolution. After acquisition, PA and US data are sampled at a rate

of 40 and 20 MHz respectively and processed further in the GPU to display interleaved pulse echo US, PA, and sO_2 images in real-time. sO_2 calculation in the AcousticX system utilizes linear unmixing strategy using 750 and 850 nm PA images without any fluence compensation, thus providing only a relative estimate.

2.2 Phantom experiments

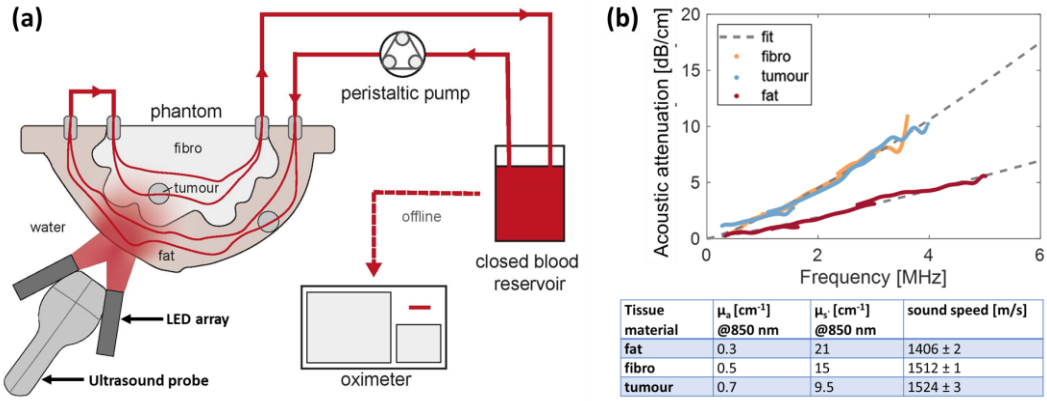

Tissue material	μ_a [cm^{-1}] @850 nm	μ_s' [cm^{-1}] @850 nm	sound speed [m/s]
fat	0.3	21	1406 ± 2
fibro	0.5	15	1512 ± 1
tumour	0.7	9.5	1524 ± 3

Figure 2. (a) Schematic of the phantom experiment for evaluating potential of LED-based PA and US imaging in breast imaging (Phantom, US probe and LED arrays were placed in a water tank) and (b) detailed optical and acoustic properties of the 3D breast phantom.

To validate the potential of AcousticX in breast imaging, we first performed an experimental study using a multi-layered sophisticated breast phantom platform with semi-anthropomorphic distribution of optical and acoustic properties and wall-less channels for mimicking blood vessels[23,24]. In this 3D breast phantom, one can tune the sO_2 of blood and test the functional imaging capability of any PA systems. Because of the breast-mimicking acoustic and optical properties of the tissue mimicking materials, this phantom is useful for evaluating dual-mode PA and US systems like AcousticX. For testing vasculature and sO_2 imaging, we filled the phantom with fresh bovine blood obtained from a slaughterhouse (fibrisol was used as an anticoagulant) one day after butchering. Sodium hydrosulfite powder was added to the blood reservoir for deoxygenation of the blood. Three different levels of sO_2 were used in this study (62.9%, 80.3%, and 96.9%) and these were measured and confirmed immediately after the PA imaging experiment using a commercial oximeter (AVOXimeter, 1000 E, ITC). Schematic of the experimental setup is shown in Fig. 2(a) and the optical and acoustic properties of the phantom are included in Fig. 2(b). Multiple experiments were conducted using this phantom to evaluate the potential of AcousticX in obtaining structural (fat-fibroglandular tissue interface, tumour morphology) and functional information (vascular density, sO_2) from breast tissue. The frame rates (combined US+PA) of 10 and 6 Hz were used for vasculature and sO_2 imaging, respectively.

2.3 Human volunteer experiment

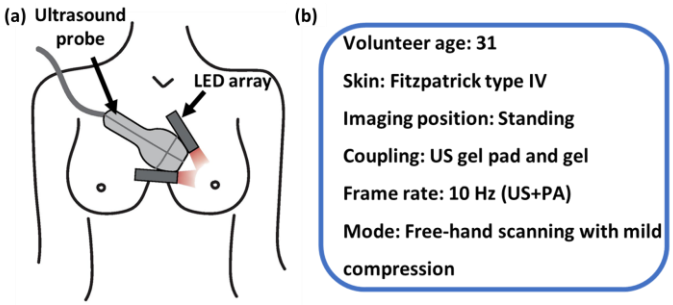

Figure 3. (a) Schematic of the breast imaging experiment on a human volunteer in which gel-pad was used for acoustic coupling during the handheld scanning, and (b) experimental settings and details of the volunteer.

For validating the *In vivo* breast imaging potential of AcousticX, we performed imaging experiment on the left breast of a human volunteer (age: 31) with Fitzpatrick type IV skin. Experimental set-up and details are shown

schematically in Fig. 3(a-b) where free-hand PA and US scanning (frame rate: 10 Hz) was performed when the volunteer was in standing position. US gel pad was used for acoustic coupling between the breast tissue and PA/US probe. Main goal of this experiment was to obtain an idea about the maximum imaging depth one can achieve in human breast tissue *in vivo*, when using AcousticX. We used 850 nm LED arrays along with the 7 MHz US probe to probe vasculature and structural details in the breast tissue.

3. RESULTS AND DISCUSSION

3.1 Phantom results – Imaging breast tumour vasculature

Figure 4(a-b) shows US and US/PA overlay images of the breast phantom. They were acquired at a location where the four blood vessels present in phantom's fat layer were inside the imaging plane. In the US image, the fat layer and fat-fibroglandular tissue interface are clearly visualized. PA images offered good vascular detectability and all four blood vessels running through the fat layer are clearly visible with high contrast (red arrows). Apart from this, the phantom's surface (green arrow) is also visible in the PA image caused by optical absorption in this layer of the phantom. Figure 4(c-d) shows US and US/PA overlay images of the phantom where tumour and its feeding blood vessel fall within the imaging plane of the probe. The structure/volume of tumour and the large feeding blood vessel as an anechoic feature are visible in the US image. Once again in this case, PA image offered excellent vascular contrast by visualizing the large feeding blood vessel as a two-walled feature as expected in a limited-view setup. These results give a direct indication that LED-PA and US imaging holds potential in imaging breast tumor morphology and vascularity with high spatial and temporal resolution.

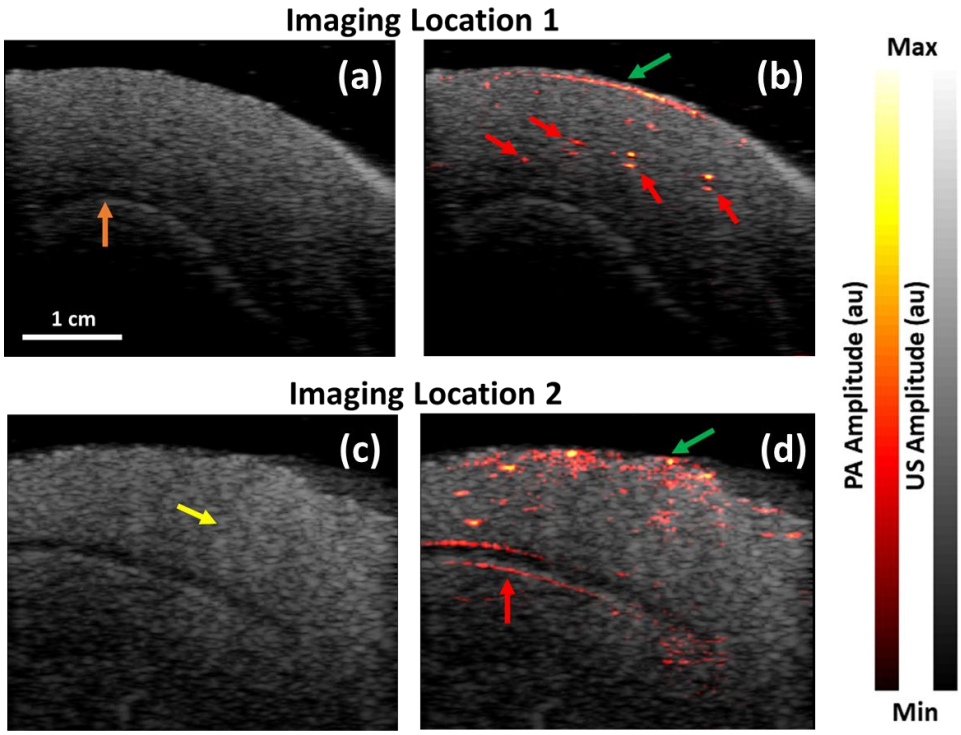

Figure 4. (a-b) shows the US and US/PA overlay images at a phantom location where four blood vessels in the fat layer were visualized along with the skin and fat-fibroglandular tissue interface, (c-d) shows US and US/PA overlay images of another phantom location at which skin, tumor and its feeding blood vessel are in the imaging plane. Green arrow: skin, Red arrow: blood vessels, Yellow arrow: Tumour, and Orange arrow: Fat-fibroglandular interface.

3.2 Phantom results – PA-based sO_2 imaging

Figure 5 (a-c) shows combined PA-based sO_2 and US images of the phantom where four blood vessel features are clearly visible in the fat layer of breast phantom at three different blood sO_2 levels (62.9, 80.3 and 96.9 %). It is evident from the

results that the PA-based sO_2 estimation was close to the actual sO_2 level for all three measurements (comparison of true sO_2 and PA-estimated sO_2 is shown in Fig. 5 (d)). Ideally, at an instance, all four blood vessel features must provide same sO_2 number. However, linear unmixing based sO_2 estimation in the system does not consider depth dependent fluence variations and also US probe sensitivity laterally. These along with the background noise in PA images may have caused slight differences in the estimate of different channels. It is worth mentioning that, on an average, error in PA-based sO_2 estimates was less than 6 %. While detecting hypoxia in malignant tumors, absolute quantification of sO_2 may not be a necessity and key factor is to get a relative estimate when compared to surrounding tissue. It is clear from our results that this is possible using LED-based PA and US imaging. US-informed fluence compensation methods may also be used in future for improving the quantitative nature of sO_2 estimates in real-time[19,25].

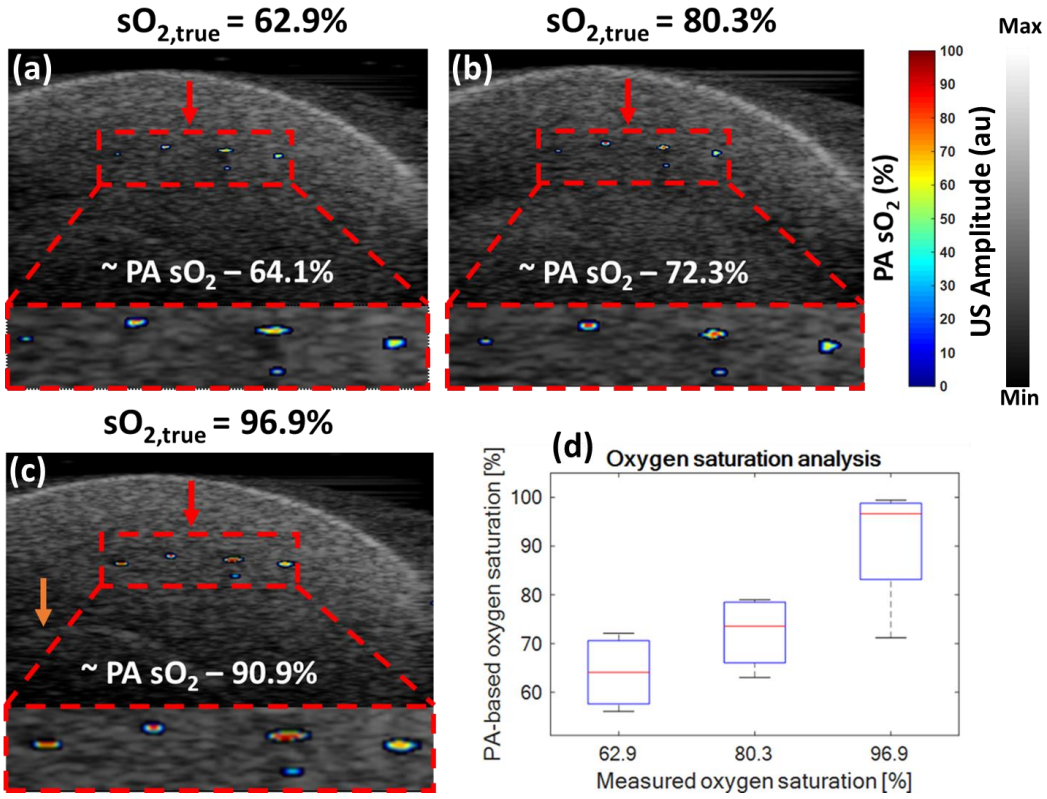

Figure 5. (a-c) shows combined PA-based sO_2 and US images of the phantom where four blood vessel features are clearly visible in the fat layer of breast phantom at three different blood sO_2 levels (62.9, 80.3 and 96.9 %), and (d) shows the comparison of PA-estimated sO_2 and actual sO_2 measured using an oximeter. Red arrow: blood vessels, Orange arrow: Fat-fibroglandular interface.

3.3 Human volunteer results – PA and US imaging of a healthy breast

Figure 6 (a) and (b) shows US and US/PA overlay images of a healthy human left breast acquired using AcousticX. During free-hand scanning of the breast in real-time, this imaging plane was randomly selected based on the number of PA-features visible in the image. Just as in the phantom experiment, US image offered good structural contrast by clearly visualizing skin, fat, fibro-glandular tissue, and pectoral muscles, which were confirmed with clinical echo images of a healthy breast[26]. On the other hand, PA image offered vascular contrast (marked using red arrows) by visualizing multiple features deep inside breast tissue. PA signal from the skin surface is quite high and this is anticipated considering the dusky complexion of the volunteer (high melanin content is expected). Deepest PA feature visible was in the pectoral muscle region at a depth of around 1.7 cm, where quite a lot of blood is expected. To the best of our knowledge, this is the highest reported imaging depth in LED-based PA imaging when using a 7 MHz US probe. The depth of penetration achieved in this study is encouraging because of low optical energy used for tissue illumination (in µJ range when compared to tens of mJ per pulse in laser-based systems). Also, it is important to discuss that we used 7 MHz US probe with an average spatial resolution of around 300 µm in all the experiments. We believe that such high

resolution is not an absolute requirement in breast cancer imaging, and we foresee to improve the imaging depth further by developing new low frequency broadband US probes and novel artificial intelligence-based image/data processing techniques[27-29].

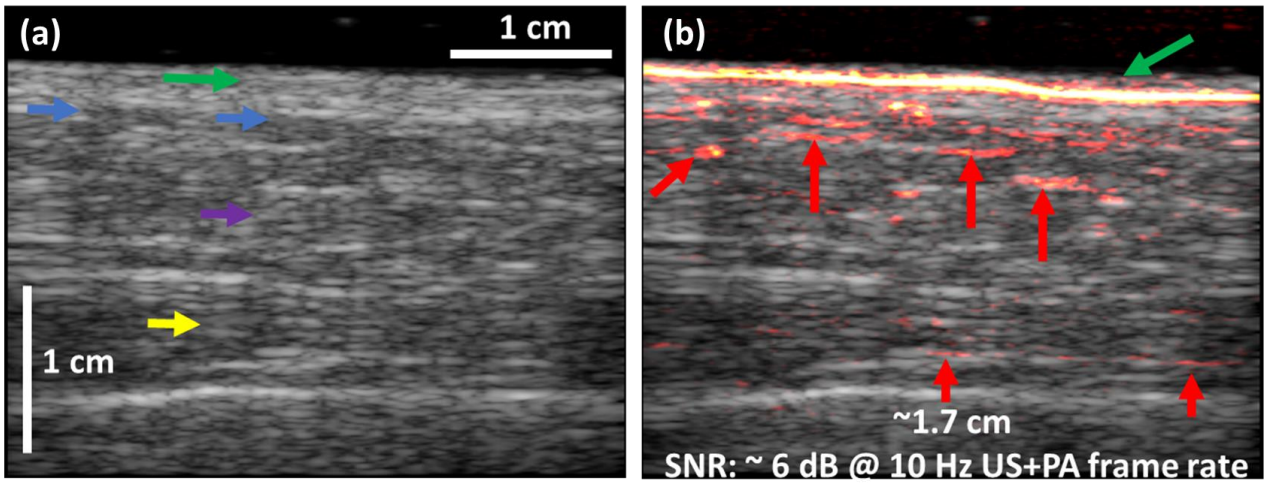

Figure 6. (a) Pulse echo US image of the left breast of a healthy volunteer, and (b) US/PA overlay image displaying structural and vascular features. Green arrow: skin, Red arrow: blood vessels, Yellow arrow: Pectoral muscle, Blue arrow: Fat, Purple arrow: Fibro-glandular tissue.

4. CONCLUSIONS AND OUTLOOK

Results of this proof-of-concept study give a direct confirmation that LED-based PA and US imaging can provide structural and functional information of breast tissue until a depth of around 1.7 cm (spatial resolution: ~ 300 µm) in real-time and thus holds clinical translation potential in non-invasive breast imaging. A portable and affordable dual-mode PA and US imaging system with capability to provide vascular patterns, tumour oxygen status and morphology is expected to have good impact in breast cancer screening in resource limited settings. In future, we plan to improve illumination (more LED elements providing uniform illumination on breast target) and acoustic detection (low frequency probe development) strategies to increase the imaging depth.

5. REFERENCES

[1] Sung, H; Ferlay, J; Siegel, RL; Laversanne, M; Soerjomataram, I; Jemal, A; and Bray, F; "Global Cancer Statistics 2020: GLOBOCAN Estimates of Incidence and Mortality Worldwide for 36 Cancers in 185 Countries," CA Cancer J Clin. (2020).

[2] Sharma, R; "Global, regional, national burden of breast cancer in 185 countries: evidence from GLOBOCAN 2018," Breast Cancer Res Treat. (2021).

[3] National Research Council; "Mammography and Beyond: Developing Technologies for the Early Detection of Breast Cancer," National Academies Press (2001).

[4] Pediconi, F; Catalano,C; Roselli, A; Dominelli, V; Cagioli, S; Karatasiou, A; Pronio, A; Kirchin, M.A.; and Passariello, R; " The challenge of imaging dense breast parenchyma: is magnetic resonance mammography the technique of choice? A comparative study with x-ray mammography and whole-breast ultrasound," Invest Radiol. 44(7):412-21 (2009).

[5] Hooley, R.J.; Andrejeva, L; and Scoutt, L.M.; "Breast cancer screening and problem solving using mammography, ultrasound, and magnetic resonance imaging," Ultrasound Q. 27(1):23-47 (2011).

[6] Onesti, J.K.; Mangus, B.E.; Helmer, S.D.; and Osland, J.S.; "Breast cancer tumor size: correlation between magnetic resonance imaging and pathology measurements," Am. J. Surg., 196 (6) (2008).

[7] Hanahan, D; and Weinberg, R.A.; "Hallmarks of cancer: the next generation." Cell, 144 (5) (2011).

[8] Tromberg, B.J.; Pogue, B.W.; Paulsen, K.D.; Yodh, A.G.; Boas, D.A.; and Cerussi, A.E.; "Assessing the future of diffuse optical imaging technologies for breast cancer management," Med. Phys., 35 (6), pp. 2443-2451 (2008).

[9] Xu, M. and Wang, L. V., “Photoacoustic imaging in biomedicine,” Review of Scientific Instruments 77(4), 041101 (2006).
[10] Manohar, S; and Dantuma, M ; “Current and future trends in photoacoustic breast imaging,” Photoacoustics, Vol. 16 (100134) (2019).
[11] Singh, M. K. A., Steenbergen, W., and Manohar, S., “Handheld probe-based dual mode ultrasound/photoacoustics for biomedical imaging,” Frontiers in Biophotonics for Translational Medicine , 209–247 (2016).
[12] Dogan, B.E.; Menezes,G.L.G.; Butler.R.S.; Neuschler, E.I.; Aitchison, R; Lavin, P.T.; Tucker, F.L.; Grobmyer, S.R.; Otto, P.M.; and Stavros, A.T.; “ Optoacoustic Imaging and Gray-Scale US Features of Breast Cancers: Correlation with Molecular Subtypes,” Radiology 292:3, 564-572 (2019).
[13] Singh, M. K. A., Sato, N., Ichihashi, F., and Sankai, Y., “Clinical translation of photoacoustic imaging—opportunities and challenges from an industry perspective,” in [LED-Based Photoacoustic Imaging], 379–393, Springer (2020).
[14] Hariri, A., Zhao, E., Jeevarathinam, A. S., Lemaster, J., Zhang, J., and Jokerst, J. V., “Molecular imaging of oxidative stress using an led-based photoacoustic imaging system,” Scientific reports 9(1), 1–10 (2019).
[15] Jo, J., Xu, G., Zhu, Y., Burton, M., Sarazin, J., Schiopu, E., Gandikota, G., and Wang, X., “Detecting joint inflammation by an led-based photoacoustic imaging system: a feasibility study,” Journal of biomedical optics 23(11), 110501 (2018).
[16] J Francis, K. J., Boink, Y. E., Dantuma, M., Singh, M. K. A., Manohar, S., and Steenbergen, W., “Tomographic imaging with an ultrasound and led-based photoacoustic system,” Biomedical Optics Express 11(4), 2152–2165 (2020).
[17] Agrawal, S., Kuniyil Ajith Singh, M., Johnstonbaugh, K., C Han, D., R Pameijer, C., and Kothapalli, S.-R., “Photoacoustic imaging of human vasculature using led versus laser illumination: A comparison study on tissue phantoms and in vivo humans,” Sensors 21(2), 424 (2021).
[18] Agrawal, S., Fadden, C., Dangi, A., Yang, X., Albahrani, H., Frings, N., Heidari Zadi, S., and Kothapalli, S.-R., “Light-emitting-diode-based multispectral photoacoustic computed tomography system,” Sensors 19(22), 4861 (2019).
[19] Bulsink, R., Kuniyil Ajith Singh, M., Xavierselvan, M., Mallidi, S., Steenbergen, W., and Francis, K. J., “Oxygen saturation imaging using led-based photoacoustic system,” Sensors 21(1), 283 (2021).
[20] Xavierselvan, M.; Singh, M.K.A.; Mallidi, S; " In Vivo Tumor Vascular Imaging with Light Emitting Diode-Based Photoacoustic Imaging System,", Sensors 20 (16), 4503 (2020).
[21] Maneas, E.; Aughwane, R.; Huynh, N.; Xia, W.; Ansari, R.; Singh, M.K.A.; Hutchinson, J.C.; Sebire, N.J.; Arthurs, O.J.; Deprest, J.; et al "Photoacoustic imaging of the human placental vasculature," J. Biophotonics 13, e201900167 (2019).
[22] Francis, K.J.; Booijink, R.; Bansal, R.; Steenbergen, W; "Tomographic Ultrasound and LED-Based Photoacoustic System for Preclinical Imaging," Sensors 20, 2793 (2020).
[23] Dantuma, M; Dommelen, R; and Manohar, S; "Semi-anthropomorphic photoacoustic breast phantom," Biomed. Opt. Express 10, 5921-5939 (2019).
[24] Dantuma, M; Kruitwagen, S; Julia, J.O.; Meerdervoort, R.P.; and Manohar, S; "Tunable blood oxygenation in the vascular anatomy of a 2 semi-anthropomorphic photoacoustic breast phantom", in press, Journal of Biomedical Optics (2021).
[25] Han, T., Yang, M., Yang, F., Zhao, L., Jiang, Y., and Li, C; “A three-dimensional modeling method for quantitative photoacoustic breast imaging with handheld probe,” Photoacoustics, 21, 100222 (2021).
[26] https://radiologyassistant.nl/breast/ultrasound/ultrasound-of-the-breast
[27] Singh, M. K. A., Sivasubramanian, K., Sato, N., Ichihashi, F., Sankai, Y., and Xing, L., “Deep learning-enhanced led-based photoacoustic imaging,” Photons Plus Ultrasound: Imaging and Sensing 2020 11240,1124038 (2020).
[28] Chandramoorthi, S.; and Thittai, A.K; "Enhancing Image Quality of Photoacoustic Tomography Using Sub-Pitch Array Translation Approach: Simulation and Experimental Validation," IEEE Trans. Biomed. Eng 66, 3543–3552 (2019).
[29] Mozaffarzadeh, M.; Hariri, A.; Moore, C.; Jokerst, J.V; "The double-stage delay-multiply-and-sum image reconstruction method improves imaging quality in a LED-based photoacoustic array scanner," Photoacoustics 12, 22–29 (2018).